



Published in final edited form as:

J Orthop Res. 2013 August ; 31(8): 1218–1225. doi:10.1002/jor.22362.

Atomic Force Microscopy Reveals Regional Variations in the Micromechanical Properties of the Pericellular and Extracellular Matrices of the Meniscus

Johannah Sanchez-Adams¹, Rebecca E. Wilusz^{1,2}, and Farshid Guilak^{1,2,*}

¹Department of Orthopaedic Surgery, Duke University Medical Center, Durham, NC, United States

²Department of Biomedical Engineering, Duke University, Durham, NC, United States

Abstract

Regional variations in the composition and architecture of the extracellular matrix (ECM) and pericellular matrix (PCM) of the knee meniscus play important roles in determining the local mechanical environment of meniscus cells. In this study, atomic force microscopy was used to spatially map the mechanical properties of matched ECM and perlecan-labeled PCM sites within the outer, middle, and inner porcine medial meniscus, and to evaluate the properties of the proximal surface of each region. The elastic modulus of the PCM was significantly higher in the outer region (151.4±38.2 kPa) than the inner region (27.5±8.8 kPa), and ECM moduli were consistently higher than region-matched PCM sites in both the outer (320.8±92.5 kPa) and inner (66.1±31.4 kPa) regions. These differences were associated with a higher proportion of aligned collagen fibers and lower glycosaminoglycan content in the outer region. Regional variations in the elastic moduli and some viscoelastic properties were observed on the proximal surface of the meniscus, with the inner region exhibiting the highest moduli overall. These results indicate that matrix architecture and composition play an important role in the regional micromechanical properties of the meniscus, suggesting that the local stress-strain environment of meniscal cells may vary significantly among the different regions.

Keywords

Chondron; fibrochondrocyte; AFM; type VI collagen; fibrocartilage

Introduction

The knee meniscus is a fibrocartilaginous tissue that provides stability within the joint, while also bearing and transmitting loads during normal locomotion. In response to joint loading, its semi-circular wedge shape increases congruence between the convex femoral condyle and relatively flat tibial plateau, resulting in an inhomogeneous stress-strain distribution

*Corresponding Author: 375 Medical Sciences Research Bldg., Box 3093 DUMC, Durham, NC 27710 Phone: 919-684-2521 Fax: 919-681-8490 guilak@duke.edu.

The authors have no conflicts to disclose.

within the tissue. Finite element models of the meniscus suggest that compressive forces dominate in the thinnest part of the wedge shape (inner region), while the thicker, more peripheral regions bear most of the circumferential tensile loads.¹⁻⁴ This complex mechanical environment is reflected in marked regional variations in cell morphology and phenotype, matrix composition, and macroscale mechanical properties.⁵⁻⁸ The periphery of the tissue, termed the outer region, contains predominantly collagen type I and fibroblast-like cells, whereas the inner region shows similarities to hyaline cartilage, with rounded cells and a relative abundance of sulfated glycosaminoglycans (GAGs) and collagen type II.^{6,9,10} Lineage tracing of collagen type II expressing cells during knee joint development has shown that in the medial meniscus these cells populate only the inner region, indicating that this tissue arises from at least two different cell populations.¹¹ Thus, the development and maintenance of these inhomogeneous properties appear to arise from differences in the biological activities of subpopulations of meniscal cells and potentially their response to the local mechanical environment.¹²

Meniscus cells are surrounded by a pericellular matrix (PCM), which together with the enclosed cells has been termed the “fibrochondron,”¹³ analogous to the “chondrons” identified in articular cartilage.¹⁴ Significant evidence suggests that the properties of this region may influence how these cells perceive mechanical and biochemical signals.¹⁵ The articular cartilage PCM, as defined by the presence of type VI collagen,¹⁶ displays a lower elastic modulus than the surrounding extracellular matrix (ECM)¹⁷ and has a significant influence on dynamic stress-strain and fluid flow environment of the chondrocytes.¹⁸ Similarly, finite element models of regional mechanics in the meniscus suggest that the mechanical environment of meniscal cells is highly dependent on region-specific properties of the tissue surrounding the cells.¹⁹ While the meniscus PCM also contains abundant collagen type VI and perlecan,^{13,20} its mechanical properties have not been previously reported. An improved understanding of the response of the meniscus to normal and pathological loading may provide important insights into the development of new strategies for regeneration or repair of the tissue. Of particular interest is an improved understanding of the regional variations in meniscal mechanotransduction, given the limited ability of the inner region for repair following injury,²¹ as well as the region-specific response of meniscal cells to tensile²² or compressive²³ mechanical stimuli.

The objective of this study was to compare the regional mechanical properties of meniscus PCM and ECM using atomic force microscopy (AFM). We hypothesized that: 1) the PCM in all regions of the meniscus has a lower modulus than its respective ECM, and 2) ECM and PCM properties vary regionally in the meniscus. To further measure mechanical inhomogeneity of the tissue, we examined ECM micromechanical properties of the proximal meniscal surface in the inner, middle, and outer regions, hypothesizing that the meniscus also exhibits regional variations in surface mechanical properties. As the local mechanical environment of meniscus cells likely plays a major role in meniscus mechanotransduction, the results from this study sought to provide key advances in micromechanical characterization of these structures in meniscus tissue.

Methods

Sample preparation

Medial menisci were harvested from skeletally mature female pigs immediately post mortem (N=3). Porcine menisci were chosen for study as they have been used extensively as a model for human menisci due to their similarity in structure and vasculature.²⁴ Both regional micromechanics of meniscus PCM and ECM and regional superficial layer micromechanics were tested. To prepare samples for both purposes, the central portion of each medial meniscus was dissected from the tissue, separated into inner, middle, and outer regions (Figure 1a-c), and frozen in cryopreservation medium with liquid nitrogen. Additionally, meniscus cross-sections were fixed and embedded in paraffin for histological analysis.

Histology and immunohistochemistry

Paraffin embedded cross-sections of medial menisci were sectioned at 10 μm and stained histologically for the presence of sulfated GAGs and collagen using Safranin-O/Fast Green. Sections were also immunohistochemically labeled for the presence and distribution of collagen types I (90395, Abcam), II (11-116B3, Developmental Studies Hybridoma Bank) and VI (70R-CR009X, Fitzgerald), as well as perlecan (Clone A7L6, Santa Cruz Biotechnology). For immunostaining, primary antibodies were incubated with the sections for 1 hour, followed by a 30 minute incubation with an appropriate biotinylated secondary antibody (ab97021, ab6844, ab6720, Abcam). Immunostaining was visualized using an AEC substrate (Invitrogen), and all sections were counterstained with Harris' hematoxylin for nuclear identification.

Micromechanics of PCM and ECM

Each meniscus region (inner, middle, outer) was cryosectioned at 5 μm , washed gently with PBS, and immunofluorescently labeled for perlecan, which has been shown previously to be localized to pericellular regions in the meniscus.²⁰ Elastic moduli were evaluated in labeled sections using an AFM (MFP-3DBio, Asylum Research) integrated with a fluorescence microscope (AxioObserver A1, Zeiss). AFM elastic mapping²⁵ was performed using spherically-tipped cantilevers (5 μm diameter; $k = 7.5 \text{ N/m}$; (Novascan)) and a force trigger of 200 nN (Figure 1b and d). PCM and ECM properties were evaluated as described previously,²⁶ with PCM sites identified by positive pericellular labeling for perlecan and ECM sites identified by a lack of perlecan staining. In each meniscus region, 16-20 site-matched ECM and PCM sites were tested. Force-indentation curves were analyzed using a modified Hertz model to determine the elastic modulus of both ECM and PCM sites, as previously reported.²⁷ A Poisson's ratio of 0.04 was used to describe both ECM and PCM sites, based on previous cartilage micromechanics measurements.^{25,28} To evaluate PCM properties, fluorescence images, height maps, and elastic moduli contour maps were aligned and analyzed as previously described.²⁶ All indentation data within labeled regions of the PCM were averaged to generate an average modulus for each PCM site (Figure 3).

AFM imaging

Cryosections of each region were also taken for AFM imaging. 5 μm sections were washed gently with deionized water and allowed to dry. Images of ECM and PCM regions were obtained on an AFM using a pyramidal tipped cantilever ($k = 42 \text{ N/m}$). $4 \times 4 \mu\text{m}$ regions were imaged in tapping mode (0.2 Hz scan rate). For PCM imaging, the scan box was set at the edge of the cell void, and for ECM imaging the scan box was set away from any cell voids.

ECM alignment quantification

AFM images of ECM sites within each meniscus region were quantified for alignment. Three amplitude images from each region were processed to achieve a black and white representation (Photoshop), and fast discrete curvelet transform analysis²⁹ was then used to detect edges in the images and the coefficient of alignment of the detected edges (CurveAlign MATLAB toolbox, Developer: Carolyn Pehlke). Coefficients of alignment were averaged within each region to give an overall description of extracellular matrix organization.

Proximal surface micromechanics

The elastic and viscoelastic properties of the surface of the inner, middle, and outer regions of the meniscus were tested using AFM techniques. Samples were prepared by dissecting the proximal surface from each region of the tissue (Figure 1c and e). These samples were then fixed to a glass slide, and hydrated with PBS. Elastic and viscoelastic tests were performed on each meniscus region using a spherically-tipped cantilever (5 μm diameter; $k = 7.5 \text{ N/m}$; (Novascan)). For both elastic and viscoelastic tests, a trigger force of 200 nN and approach velocity of 15 $\mu\text{m/s}$ were used. Elastic curves were sampled at 7.5 kHz, and viscoelastic curves were sampled at $\sim 400 \text{ Hz}$ for 60 seconds. Elastic curves ($n=30$) were analyzed as described for PCM/ECM micromechanics, accounting for the larger tip diameter. Viscoelastic curves ($n=10$) were analyzed as described in our previous work³⁰ to determine the equilibrium modulus (E_∞), instantaneous modulus (E_0), time constants (τ_σ and τ_ϵ), and viscosity (μ) of each sample.

Statistical Analysis

PCM and ECM force mapping data was analyzed using a two-way ANOVA (matrix type, meniscus region), and a Fisher's LSD post-hoc test was used for individual comparisons, if warranted ($\alpha = 0.05$). Proximal superficial layer mechanical properties were analyzed using a one-way ANOVA (meniscus region), with a Fisher's post-hoc test ($\alpha = 0.05$).

Results

Histology and immunohistochemistry

Porcine medial menisci displayed regional differences in labeling for sulfated GAGs, collagen type I, and collagen type II (Figure 2). Sulfated GAGs and collagen type II were most abundant in the inner PCM and ECM areas of the meniscus. Collagen type I was most abundant in the outer and middle regions, and was less abundant in the inner ECM and PCM. Collagen type VI and perlecan were found throughout the meniscus, though perlecan

appeared confined to the PCM whereas collagen type VI resided in the ECM and PCM. A thin, 8-10 μm acellular surface layer of matrix was also observed.

Micromechanical properties of the PCM and ECM

The PCM modulus in the outer region of the meniscus was significantly higher than both the middle and inner PCM moduli (Figure 4). Additionally, the inner region of the meniscus showed the lowest overall modulus when considering both ECM and PCM data, with the middle and outer regions showing the next highest and highest overall moduli, respectively. The PCM in all regions displayed a lower modulus than the local ECM. Individual comparisons showed that in the outer region, the PCM (151.4 ± 38.2 kPa) modulus was 52.8% lower than that of the ECM (320.8 ± 92.5 kPa). Similarly, the PCM in the inner region displayed a 58.4% lower modulus than the ECM (27.5 ± 8.8 kPa and 66.1 ± 31.4 kPa, respectively). The greatest difference in PCM and ECM modulus was found in the middle region, where the PCM showed a 78.2% lower modulus than the ECM (54.9 ± 27.3 kPa and 252.1 ± 83.3 kPa, respectively).

AFM imaging and alignment quantification

Representative AFM images for outer, middle, and inner ECM and PCM regions are shown in Figure 5. ECM sites in the outer and middle regions displayed thick collagen fibrils whereas similar sites in the inner region showed less distinct collagen fibrils. PCM sites in the inner and middle regions also displayed a smoother appearance with less prominent collagen fibrils while the outer PCM sites displayed more distinct collagen fibrils. Quantification of ECM alignment showed the highest coefficient of alignment in the outer region (0.77 ± 0.06), while the inner region (0.51 ± 0.15) displayed a statistically lower coefficient of alignment (Figure 6). The middle region coefficient of alignment (0.60 ± 0.18) was not statistically different from the other regions.

Proximal surface micromechanics

The surface of the meniscus displayed regionally varying elastic and viscoelastic properties. A statistically higher elastic modulus (Figure 7a) was found in the inner region of the meniscus (59.82 ± 14.96 kPa) compared with the outer region (35.8 ± 6.57 kPa). The middle region displayed an intermediate modulus (41.72 ± 1.15 kPa). Viscoelastic properties τ_e and μ showed a similar regional variation, but E_∞ , E_0 , and τ_σ did not vary regionally (Figure 7b-f).

Discussion

This study examined regional micromechanical properties of the knee meniscus in both the extracellular environment and in the region immediately surrounding the resident cells (i.e., the PCM). Our results support the hypotheses that both ECM and PCM elastic moduli vary significantly with region in the meniscus, and that the meniscus PCM modulus is consistently lower than the ECM modulus. AFM indentation of the superficial layer of the meniscus also revealed regional variations in both elastic and viscoelastic mechanical properties on the tissue surface. These differences in micromechanical properties of the ECM and PCM suggest that the cellular mechanical environment may be highly dependent

on the location within the tissue, potentially influencing the local response of meniscal cells to joint loading.

The lower modulus of PCM relative to ECM values (Figure 4) is consistent with trends reported for articular cartilage,²⁵ and supports previous work demonstrating that macroscopic meniscus strains are altered in the cell microenvironment.^{31,32} Moreover, as finite element modeling of meniscus loading predicts varying outer and inner meniscus cell strains,^{19,32,33} the observed regional variations in PCM mechanics suggests that this structure may differentially influence the biophysical environment perceived by cells in different regions of the tissue. For example, in articular cartilage, the PCM appears to reduce cell-level strains in superficial regions characterized by high ECM strain,³⁴ while amplifying local strains in deeper zones.³⁵ The macroscale depth-dependent strain distribution in the meniscus differs significantly from that in articular cartilage, with the highest strain observed deeper in the meniscus.³⁴ These findings suggest that in addition to the regional variations observed in PCM mechanics, depth-dependent variations will be an important variable to consider in future work. Therefore, further research on the relationship between cell, PCM, and ECM deformation in the meniscus may reveal additional insights on the PCM's role in modulating the environment of meniscal cells.

Interestingly, the PCM elastic modulus was found to vary with meniscus region (Figure 4), a characteristic distinguishing meniscus PCM from hyaline articular cartilage PCM. In articular cartilage, PCM modulus does not vary with tissue zone,^{15,26} although significant differences exist in ECM^{26,36-39} and cellular³⁰ mechanical properties with depth from the tissue surface. In the current study, the lowest meniscus PCM modulus was found in the inner region and the highest in the outer region, which parallels the measured ECM moduli trends and previously reported mechanical properties of meniscus cells.⁴⁰ The biomechanical function, if any, of these regional variations in PCM properties in the meniscus needs further investigation, but may be associated with large inhomogeneities in the stress-strain environment of the meniscus, which experiences significant tensile and compressive stresses in different regions.¹⁻⁴

The observed regional differences in ECM and PCM mechanical properties (Figure 4) are likely related to the varying composition and organization of matrix molecules throughout the meniscus.^{6,7,41} In the outer region, collagen is the predominant ECM component and is highly aligned in the circumferential direction. However, in the inner region where collagen alignment is less prominent, a higher concentration of sulfated GAGs contributes significantly to ECM composition and mechanics.⁴² At the microscale, collagen may also show a higher apparent stiffness than proteoglycan.⁴³ Differences in matrix organization were detected via analysis of AFM images in the different regions (Figure 6), and may explain why the outer region ECM was found to have a much higher modulus than the inner region. As the mechanical characterization of ECM and PCM moduli was performed in the circumferential direction, the highly organized collagen in the outer region may be stiffer in this direction than the less organized collagen of the inner region. The inner region's lower modulus is also consistent with prior AFM-based studies of the micromechanical properties of hyaline cartilage which, along the direction of collagen orientation, the GAG-rich middle and deep zones display a lower modulus compared with the less GAG-rich environment of the

superficial zone.³⁶ Thus, at the microscale it appears that cartilaginous tissues that display a high elastic modulus do so either because of highly organized collagen, lack of hydrophilic molecules such as GAGs, or a combination of the two.

Another important micromechanical aspect to consider is the proximo-distal variation in meniscus collagen architecture, as collagen organization is known to help the meniscus distribute mechanical forces.³ While collagen orientation is predominantly circumferential, a thin network of collagen fibers characterizes the tissue's surface.⁴⁴ The mechanical properties of this surface may impact force transmission through the tissue depth and may also influence nutrient exchange profiles between the synovial fluid and the different regions of the tissue during loading. Following this anisotropy in matrix organization, anisotropic mechanical properties were apparent between the circumferential and axial testing directions in the present study. In particular, a marked decrease in modulus was observed between the ECM values and the surface mechanical properties in the outer and middle regions (Figures 4 and 7), which may reflect the different testing directions (parallel vs. perpendicular to collagen fiber orientation) combined with differences in collagen fiber diameter. While the surface of the meniscus is covered by a 10 μm thick layer of randomly oriented collagen fibers of around 35 nm in diameter, the deeper core of the tissue contains highly circumferentially-aligned collagen fiber bundles of greater than 20 μm .⁴⁵ Therefore, the difference in collagen architecture on the surface of the meniscus compared with its cross-section may give rise to different compressive properties. These results suggest that meniscus mechanical anisotropy not only exists at the macroscale,⁴⁶ but also at the microscale. However, it is important to note that the circumferential measurements necessarily were made on cut surfaces, while the goal of the AFM measurements in the normal direction was to measure the properties of the intact surface of the meniscus. Additionally, trends in meniscus surface elastic modulus and some viscoelastic properties were opposite that observed in the ECM/PCM testing, with the inner region displaying the highest, and the outer region displaying the lowest mechanical properties. As the collagen orientation on the meniscus surface is known to be random in all regions, this variation in properties could reflect that mechanics in this layer may also be dominated by factors such as GAG abundance.

The present results indicate that microscale compressive properties in the meniscus using AFM are generally consistent with macroscale measures, which have reported an axial aggregate modulus ranging from 100-150 kPa under creep indentation,⁴⁷ to around 400 kPa in confined compression.⁴⁸ In the context of previous studies using microscale or nanoscale mechanical testing modes, our findings, similar to those in articular cartilage suggest that the testing configuration may significantly influence the measured properties.³⁸ For example, studies of the axial compressive properties of the 150-200 μm thick superficial layer of the meniscus using a 300 μm diameter probe have reported a steady-state modulus of around 1.67 MPa in the middle region.⁴⁹ In contrast, the equilibrium modulus of the proximal meniscus surface measured in the present study by AFM was one to two orders of magnitude lower than this value. This discrepancy may be due to the differences in applied strain to the tissue, as the present results reflect an indentation into the meniscal surface of around 1-2 μm and previous studies indent or compress the tissue by at least 8 μm . Thus, the present results likely reflect testing of only the randomly-oriented, 10 μm thick layer of

collagen enveloping the meniscus (Figure 2). This part of the tissue exhibits similar structure to the lamina splendens of articular cartilage, a thin surface layer containing a fine fibrillar network.⁵⁰ Previous findings, however, may reflect the contribution of underlying layers of more organized or larger diameter collagenous components. Therefore, this broad range of meniscus compressive properties at different size scales is likely a reflection of the hierarchical structure of the ECM. While a function for these variations in mechanical properties at different scales has yet to be determined, they are likely to influence the local deformation profile of the meniscus under loading, and presumably, the mechanical environment of cells within the tissue.¹⁹

The findings of this study provide quantitative measures of micromechanical properties of the meniscus ECM and PCM. This information is critical for developing multiscale mathematical models of cell-matrix interactions at the microscale,⁵¹ providing further insight into tissue's response to physiologic or pathological loading conditions. An improved understanding of the relationship between mechanical factors at the joint level with those at the cellular level will hopefully lead to new strategies for preventing meniscus degeneration or injury, as well as the development of new repair or regenerative approaches.

Acknowledgments

This work was supported by the Arthritis Foundation, the NSF, and NIH grants AG15768, AR48852, AR50245, and AR48182.

References

1. LeRoux MA, Setton LA. Experimental and biphasic FEM determinations of the material properties and hydraulic permeability of the meniscus in tension. *J Biomech Eng.* 2002; 124:315–321. [PubMed: 12071267]
2. Spilker RL, Donzelli PS, Mow VC. A transversely isotropic biphasic finite element model of the meniscus. *J Biomech.* 1992; 25:1027–1045. [PubMed: 1517263]
3. Beaupre A, Choukroun R, Guidouin R, et al. Knee menisci. Correlation between microstructure and biomechanics. *Clin Orthop Relat Res.* 1986:72–75. [PubMed: 3720145]
4. Pena E, Calvo B, Martinez MA, et al. Finite element analysis of the effect of meniscal tears and meniscectomies on human knee biomechanics. *Clin Biomech (Bristol, Avon).* 2005; 20:498–507.
5. Hellio Le Graverand MP, Ou Y, Schield-Yee T, et al. The cells of the rabbit meniscus: their arrangement, interrelationship, morphological variations and cytoarchitecture. *J Anat.* 2001; 198:525–535. [PubMed: 11430692]
6. McDevitt CA, Webber RJ. The ultrastructure and biochemistry of meniscal cartilage. *Clin Orthop Relat Res.* 1990:8–18. [PubMed: 2406077]
7. Vanderploeg EJ, Wilson CG, Imler SM, et al. Regional variations in the distribution and colocalization of extracellular matrix proteins in the juvenile bovine meniscus. *J Anat.* 2012; 221:174–186. [PubMed: 22703476]
8. Killian ML, Lepinski NM, Haut RC, Haut Donahue TL. Regional and zonal histo-morphological characteristics of the lapine menisci. *Anat Rec (Hoboken).* 2010; 293:1991–2000. [PubMed: 21077170]
9. Cheung HS. Distribution of type I, II, III and V in the pepsin solubilized collagens in bovine menisci. *Connect Tissue Res.* 1987; 16:343–356. [PubMed: 3132349]
10. Chia HN, Hull ML. Compressive moduli of the human medial meniscus in the axial and radial directions at equilibrium and at a physiological strain rate. *J Orthop Res.* 2008; 26:951–956. [PubMed: 18271010]

11. Hyde G, Boot-Handford RP, Wallis GA. Col2a1 lineage tracing reveals that the meniscus of the knee joint has a complex cellular origin. *Journal of Anatomy*. 2008; 213:531–538. [PubMed: 19014360]
12. Hennerbichler A, Moutos FT, Hennerbichler D, et al. Repair response of the inner and outer regions of the porcine meniscus in vitro. *Am J Sports Med*. 2007; 35:754–762. [PubMed: 17261570]
13. McDevitt, CA.; Li, H.; Zaramo, C.; Prajapati, R. The Isolation of a Cell-Pericellular Matrix Complex from Meniscus Fibrocartilage: The Fibrochondron. Orthopaedic Research Society Annual Meeting Poster #0384; 2001.
14. Szirmai, JA. Structure of Cartilage. In: Engel, A.; Larsson, T., editors. *Aging of Connective and Skeletal Tissue*. Nordiska; Stockholm, Sweden: 1969. p. 163-200.
15. Guilak F, Alexopoulos LG, Upton ML, et al. The pericellular matrix as a transducer of biomechanical and biochemical signals in articular cartilage. *Ann N Y Acad Sci*. 2006; 1068:498–512. [PubMed: 16831947]
16. Poole CA, Ayad S, Schofield JR. Chondrons from articular cartilage: I. Immunolocalization of type VI collagen in the pericellular capsule of isolated canine tibial chondrons. *J Cell Sci*. 1988; 90(Pt 4):635–643. [PubMed: 3075620]
17. Wilusz RE, Defrate LE, Guilak F. A biomechanical role for perlecan in the pericellular matrix of articular cartilage. *Matrix Biol*. 2012
18. Kim E, Guilak F, Haider MA. An axisymmetric boundary element model for determination of articular cartilage pericellular matrix properties in situ via inverse analysis of chondron deformation. *J Biomech Eng*. 2010; 132:031011. [PubMed: 20459199]
19. Upton ML, Guilak F, Laursen TA, Setton LA. Finite element modeling predictions of region-specific cell-matrix mechanics in the meniscus. *Biomech Model Mechanobiol*. 2006; 5:140–149. [PubMed: 16520958]
20. Melrose J, Smith S, Cake M, et al. Comparative spatial and temporal localisation of perlecan, aggrecan and type I, II and IV collagen in the ovine meniscus: an ageing study. *Histochem Cell Biol*. 2005; 124:225–235. [PubMed: 16028067]
21. Starke C, Kopf S, Petersen W, Becker R. Meniscal repair. *Arthroscopy*. 2009; 25:1033–1044. [PubMed: 19732643]
22. Upton ML, Hennerbichler A, Fermor B, et al. Biaxial strain effects on cells from the inner and outer regions of the meniscus. *Connect Tissue Res*. 2006; 47:207–214. [PubMed: 16987752]
23. Hennerbichler A, Fermor B, Hennerbichler D, et al. Regional differences in prostaglandin E2 and nitric oxide production in the knee meniscus in response to dynamic compression. *Biochem Biophys Res Commun*. 2007; 358:1047–1053. [PubMed: 17517372]
24. Peretti GM, Gill TJ, Xu JW, et al. Cell-based therapy for meniscal repair: a large animal study. *Am J Sports Med*. 2004; 32:146–158. [PubMed: 14754738]
25. Darling EM, Wilusz RE, Bolognesi MP, et al. Spatial mapping of the biomechanical properties of the pericellular matrix of articular cartilage measured in situ via atomic force microscopy. *Biophys J*. 2010; 98:2848–2856. [PubMed: 20550897]
26. Wilusz RE, Defrate LE, Guilak F. Immunofluorescence-guided atomic force microscopy to measure the micromechanical properties of the pericellular matrix of porcine articular cartilage. *J R Soc Interface*. 2012; 9:2997–3007. [PubMed: 22675162]
27. Darling EM, Topel M, Zauscher S, et al. Viscoelastic properties of human mesenchymally-derived stem cells and primary osteoblasts, chondrocytes, and adipocytes. *J Biomech*. 2008; 41:454–464. [PubMed: 17825308]
28. Alexopoulos LG, Williams GM, Upton ML, et al. Osteoarthritic changes in the biphasic mechanical properties of the chondrocyte pericellular matrix in articular cartilage. *J Biomech*. 2005; 38:509–517. [PubMed: 15652549]
29. Candes E, Demanet L, Donoho D, Ying LX. Fast discrete curvelet transforms. *Multiscale Modeling & Simulation*. 2006; 5:861–899.
30. Darling EM, Zauscher S, Guilak F. Viscoelastic properties of zonal articular chondrocytes measured by atomic force microscopy. *Osteoarthritis Cartilage*. 2006; 14:571–579. [PubMed: 16478668]

31. Upton ML, Gilchrist CL, Guilak F, Setton LA. Transfer of macroscale tissue strain to microscale cell regions in the deformed meniscus. *Biophys J*. 2008; 95:2116–2124. [PubMed: 18487290]
32. Gupta T, Haut Donahue TL. Role of cell location and morphology in the mechanical environment around meniscal cells. *Acta Biomater*. 2006; 2:483–492. [PubMed: 16860617]
33. Meakin JR, Shrive NG, Frank CB, Hart DA. Finite element analysis of the meniscus: the influence of geometry and material properties on its behaviour. *Knee*. 2003; 10:33–41. [PubMed: 12649024]
34. Lai JH, Levenston ME. Meniscus and cartilage exhibit distinct intra-tissue strain distributions under unconfined compression. *Osteoarthritis Cartilage*. 2010; 18:1291–1299. [PubMed: 20633686]
35. Choi JB, Youn I, Cao L, et al. Zonal changes in the three-dimensional morphology of the chondron under compression: the relationship among cellular, pericellular, and extracellular deformation in articular cartilage. *J Biomech*. 2007; 40:2596–2603. [PubMed: 17397851]
36. McLeod MA, Wilusz RE, Guilak F. Depth-dependent anisotropy of the micromechanical properties of the extracellular and pericellular matrices of articular cartilage evaluated via atomic force microscopy. *J Biomech*. 2012
37. Tomkoria S, Patel RV, Mao JJ. Heterogeneous nanomechanical properties of superficial and zonal regions of articular cartilage of the rabbit proximal radius condyle by atomic force microscopy. *Med Eng Phys*. 2004; 26:815–822. [PubMed: 15567698]
38. Huang CY, Stankiewicz A, Ateshian GA, Mow VC. Anisotropy, inhomogeneity, and tension-compression nonlinearity of human glenohumeral cartilage in finite deformation. *J Biomech*. 2005; 38:799–809. [PubMed: 15713301]
39. Schinagl RM, Gurskis D, Chen AC, Sah RL. Depth-dependent confined compression modulus of full-thickness bovine articular cartilage. *J Orthop Res*. 1997; 15:499–506. [PubMed: 9379258]
40. Sanchez-Adams J, Athanasiou KA. Biomechanics of meniscus cells: regional variation and comparison to articular chondrocytes and ligament cells. *Biomech Model Mechanobiol*. 2012; 11:1047–1056. [PubMed: 22231673]
41. Angele P, Johnstone B, Kujat R, et al. Stem cell based tissue engineering for meniscus repair. *J Biomed Mater Res A*. 2008; 85:445–455. [PubMed: 17729255]
42. Sanchez-Adams J, Willard VP, Athanasiou KA. Regional variation in the mechanical role of knee meniscus glycosaminoglycans. *J Appl Physiol*. 2011; 111:1590–1596. [PubMed: 21903884]
43. Loparic M, Wirz D, Daniels AU, et al. Micro- and nanomechanical analysis of articular cartilage by indentation-type atomic force microscopy: validation with a gel-microfiber composite. *Biophys J*. 2010; 98:2731–2740. [PubMed: 20513418]
44. Aspden RM, Yarker YE, Hukins DW. Collagen orientations in the meniscus of the knee joint. *J Anat*. 1985; 140(Pt 3):371–380. [PubMed: 4066476]
45. Petersen W, Tillmann B. Collagenous fibril texture of the human knee joint menisci. *Anat Embryol (Berl)*. 1998; 197:317–324. [PubMed: 9565324]
46. Gabrion A, Aïmedieu P, Laya Z, et al. Relationship between ultrastructure and biomechanical properties of the knee meniscus. *Surg Radiol Anat*. 2005; 27:507–510. [PubMed: 16308664]
47. Sweigart MA, Zhu CF, Burt DM, et al. Intraspecies and interspecies comparison of the compressive properties of the medial meniscus. *Ann Biomed Eng*. 2004; 32:1569–1579. [PubMed: 15636116]
48. Proctor CS, Schmidt MB, Whipple RR, et al. Material properties of the normal medial bovine meniscus. *J Orthop Res*. 1989; 7:771–782. [PubMed: 2677284]
49. Moyer JT, Abraham AC, Haut Donahue TL. Nanoindentation of human meniscal surfaces. *J Biomech*. 2012; 45:2230–2235. [PubMed: 22789734]
50. Teshima R, Otsuka T, Takasu N, et al. Structure of the Most Superficial Layer of Articular-Cartilage. *Journal of Bone and Joint Surgery-British*. 1995; Volume 77B:460–464.
51. Halloran JP, Sibole S, van Donkelaar CC, et al. Multiscale mechanics of articular cartilage: potentials and challenges of coupling musculoskeletal, joint, and microscale computational models. *Ann Biomed Eng*. 2012; 40:2456–2474. [PubMed: 22648577]

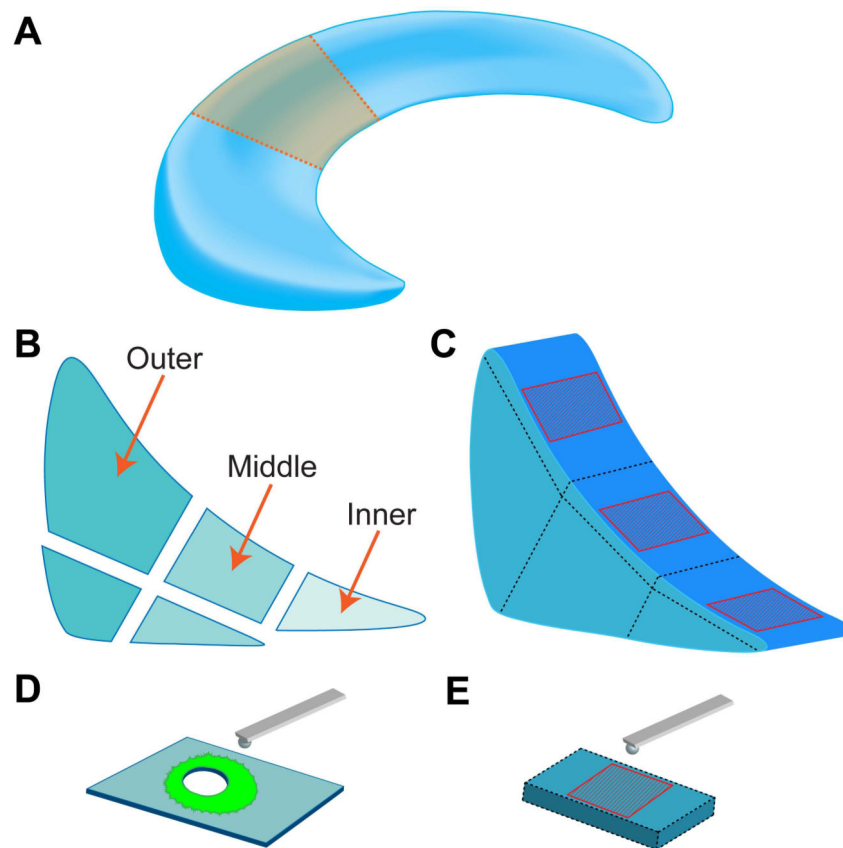


Figure 1. Meniscus testing overview

The central portion of each medial meniscus (A) was analyzed. Cross-sections (B) or the proximal superficial surface (C) of the outer, middle and inner regions were dissected. Cross-sections from (B) were cryosectioned, labeled for perlecan, and AFM force maps of PCM and ECM regions were determined (D). Following dissection, the proximal surface in each region was also mechanically tested (E).

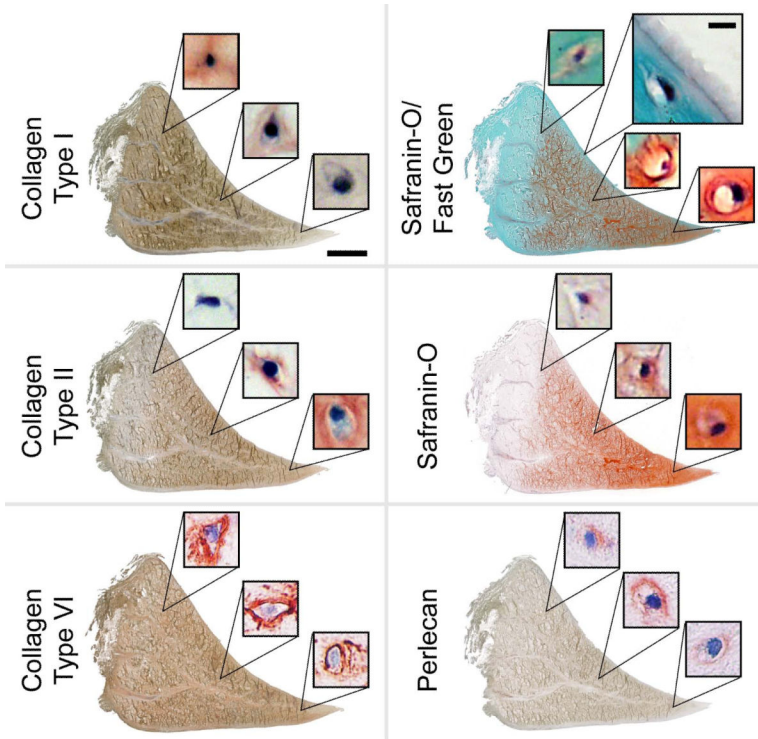


Figure 2. Regional variations in meniscus matrix molecules

Collagen types I and II show characteristic abundance in the outer and inner regions of the tissue, respectively. Sulfated GAG content was also most abundant in the inner region of the tissue, and a thin, 8-10 μm superficial layer was observed. Collagen type VI was found throughout the tissue as well as localized around meniscus cells in each region. Perlecan was less abundant, but found localized around meniscus cells. Scale bar: 20 mm; cell views: 20 \times 20 μm ; surface view: 40 \times 40 μm , 10 μm scale.

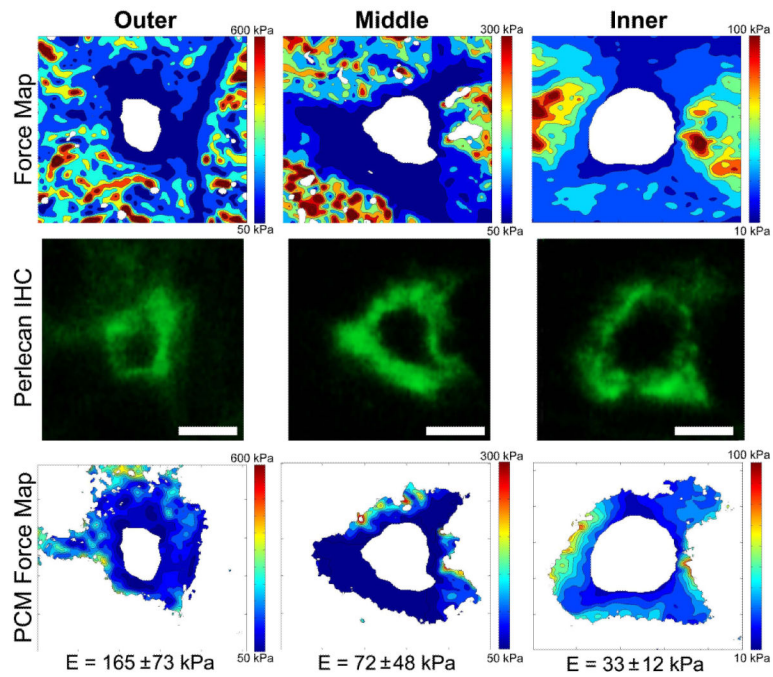


Figure 3. Integration of AFM force maps and PCM fluorescent labeling

$20 \times 20 \mu\text{m}$ force maps of pericellular sites within each meniscus region (top row) were integrated with fluorescent perlecan staining (middle row) to define PCM boundaries. The resulting PCM force maps were analyzed to yield an average elastic modulus (bottom row).

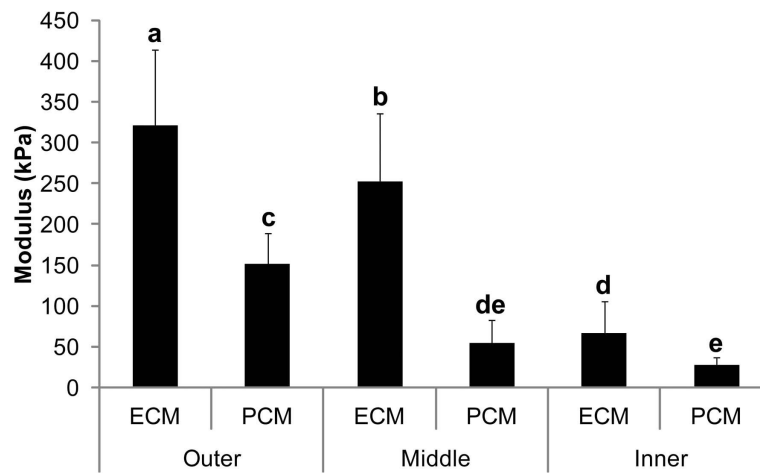


Figure 4. Regional variation of meniscus ECM and PCM elastic moduli

Elastic moduli of PCM regions was found to vary regionally in the tissue, with outer PCM sites showing a higher moduli than inner PCM sites. ECM sites were found to have consistently higher moduli than PCM sites, regardless of region. 1-way ANOVA, Fisher's post-hoc, $\alpha=0.05$. Data presented as mean \pm SD. Groups not connected by the same letter are statistically significant.

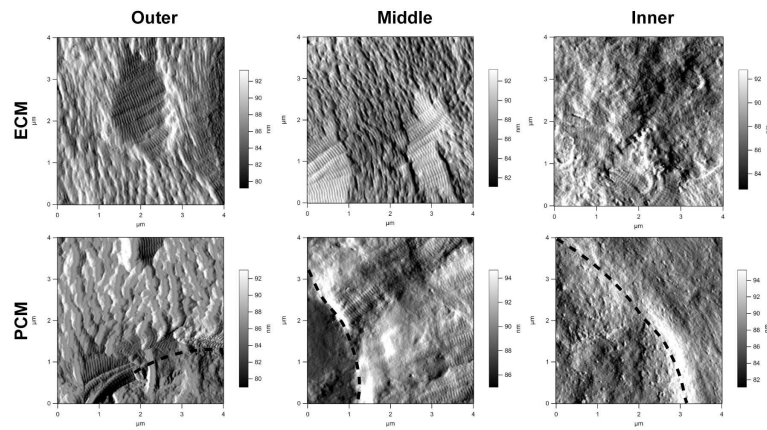


Figure 5. Regional AFM imaging of meniscus ECM and PCM sites

Outer and middle ECM sites and outer PCM sites showed more prominent collagen organization than inner ECM and inner and middle PCM sites. Images are of a $4 \times 4 \mu\text{m}$ area, and cell voids are indicated by a dashed line.

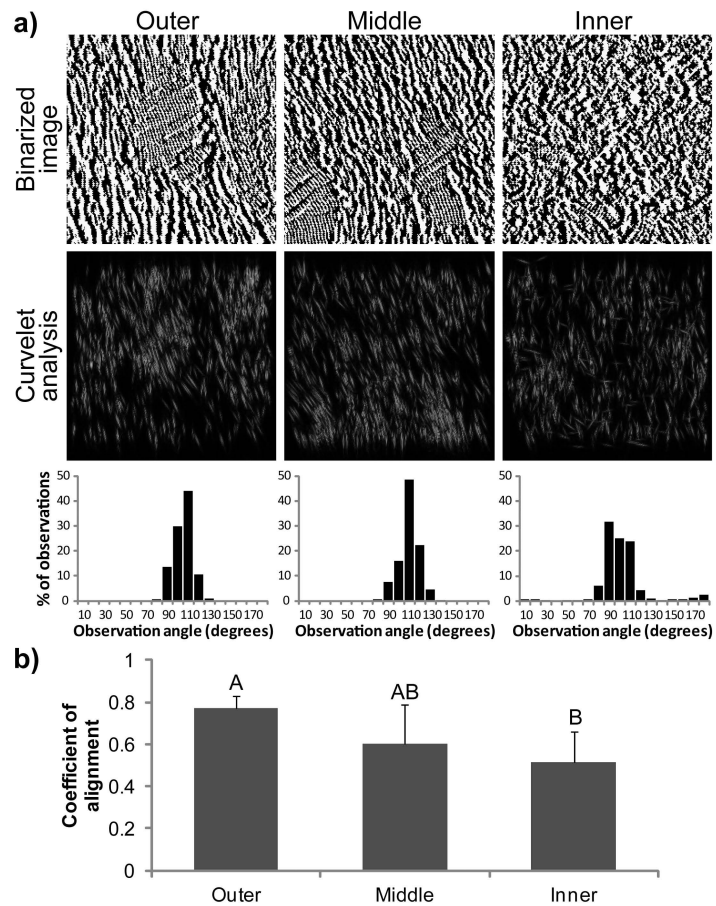


Figure 6. Quantification of alignment in AFM images

Amplitude images of ECM sites within each region were binarized (a, top row), and then analyzed with fast discrete curvelet transforms (a, second row). The resulting angles of orientation of the detected edges were recorded (a, third row). The distribution of these orientation angles were then described using a coefficient of alignment (b). 1-way ANOVA, Fisher's post-hoc, $\alpha=0.05$. Data presented as mean \pm SD. Groups not connected by the same letter are statistically significant.

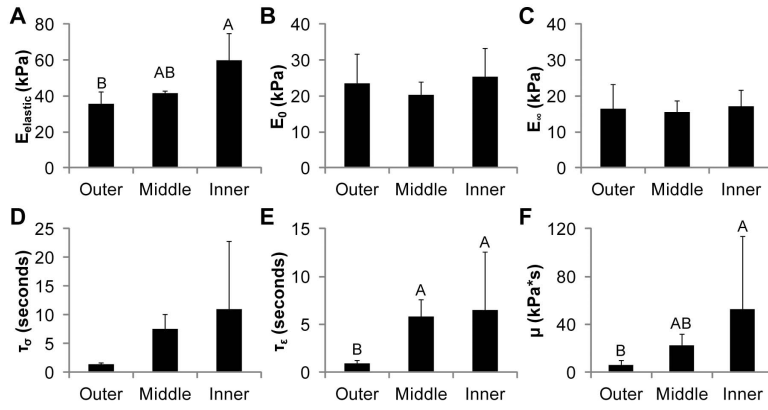


Figure 7. Elastic and viscoelastic properties of the superficial layer of the proximal surface of the meniscus

The superficial layer of the inner region displayed a statistically higher elastic modulus than the outer region superficial layer. This relationship was conserved for the viscosity (μ), and was similar for the viscoelastic time constant (τ_σ), but no trend or statistical difference in E_0 or E_∞ was detected. 1-way ANOVA, Fisher's post-hoc, $\alpha=0.05$. Data presented as mean \pm SD. Groups not connected by the same letter are statistically significant.